

## A Tentative View on Development of Tropical Disturbances

Nobuyoshi Shimizu\*  
Meteorological Satellite Center

### Abstract

Tropical upper tropospheric synoptic-scale wave disturbances, mostly caused by cut-off lows, induce corresponding lower and middle tropospheric disturbances preferentially in the region of vertical easterly shear. These synoptic-scale waves develop due to dynamic instability of the vertical shear of the tropical atmosphere.

Cloud cluster-scale motions develop spontaneously in the core regions of the synoptic-scale wave disturbances. The upward motion decreases the moist static stability and is, in turn, intensified by the decrease of moist static stability. This recurrent process eventually produces a warm core in the convectively unstable layer. The intense upward motion induces cyclonic vorticity at the lower levels and anticyclonic vorticity at the upper levels of the troposphere.

### 1. Introduction

#### 1.1 General

The question of what produces typhoons has not yet been answered clearly in spite of many years of works by many researchers. Resolution of this question is necessary for synoptic forecasters to issue reliable warnings about potential disasters. This paper, therefore, presents a tentative view on the development of pre-typhoon tropical disturbances which may aid in the study of typhoon.

Extensive classical works have been reviewed by Yanai (1964). Many synoptic features of the background environmental fields responsible for the development of tropical disturbances have been clarified by observational studies by Yanai (1961), Reed and Recker (1971), Gray (1968,1978), Frank (1977), McBride and Zehr (1981) and Lee (1989).

Numerical simulations of the formation of typhoons in convective unstable atmospheric conditions were not sufficient due to sensitivity of the governing equations to cumulus-scale motions (Kasahara 1960, Syono 1960). To overcome this problem, the idea of Conditional Instability of the Second Kind (CISK) has been successfully utilized in theoretical numerical models since it was first introduced by Charney and Eliassen (1964) and Ooyama (1964). However, CISK uses the initial disturbance as the basis of its calculations. Its genesis and the mechanism of CISK require further study in synoptic fashion to understand the development of tropical disturbances.

#### 1.2 Some aspects of environmental fields for tropical disturbances

Figure 1 is reproduced from Gray (1978). The top and bottom figures, taken from his fig.

---

\* (Received August 13 ; Revised November 9, 1993)

13 and 14, respectively, show smoothed wind fields at 200 mb and gradient level.

The middle figure, taken from his fig. 23 shows cyclone origin locations over twenty years. The

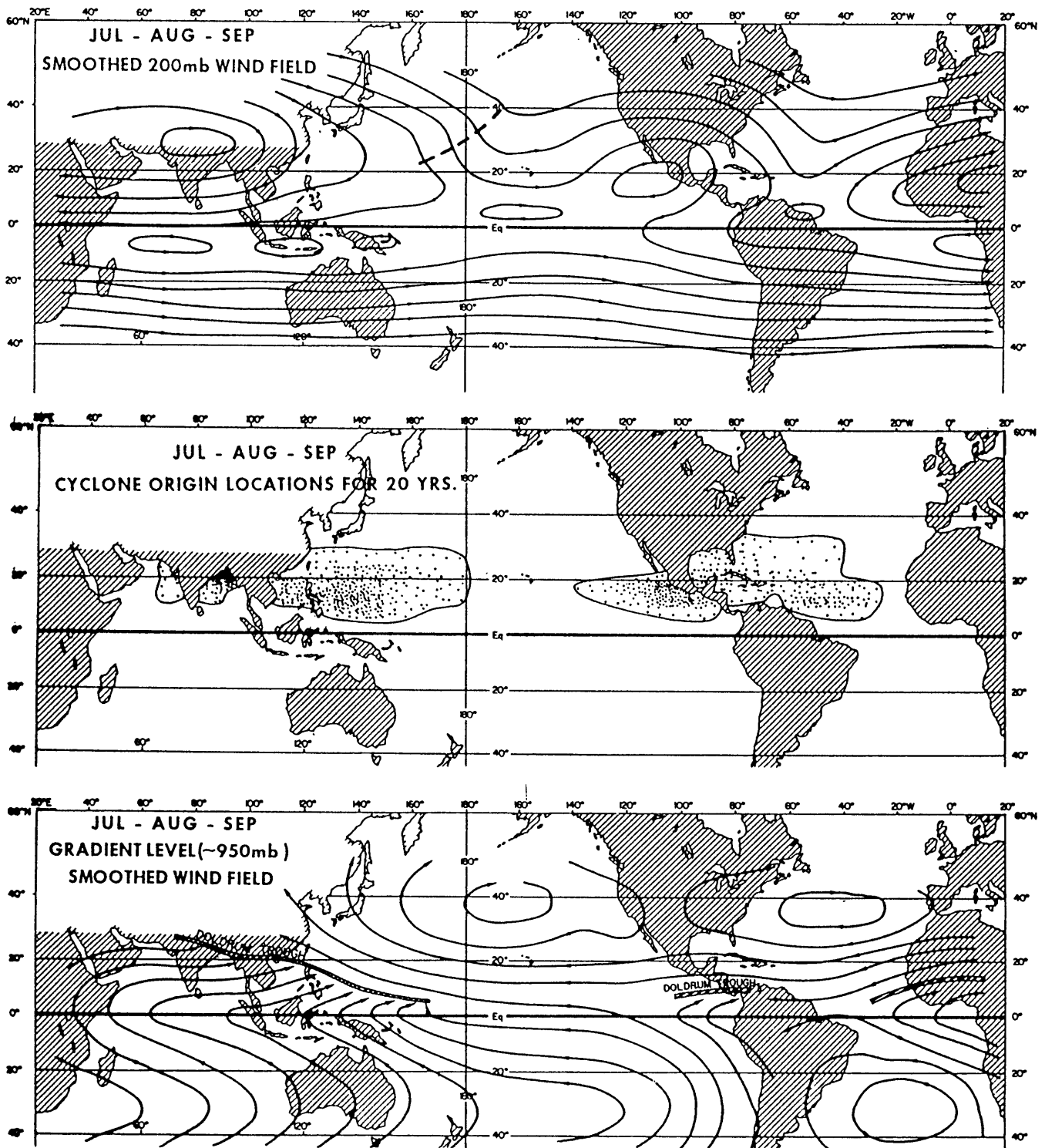


Fig.1: Smoothed wind field at 200 mb (top) and at the gradient level ~ 950 mb (bottom) during July through September and cyclone origin locations for 20 years (middle), reproduced from Gray (1978).

regions of hurricanes and typhoons are commonly characterized by the easterly and northerly components at 200 mb and the westerly and southerly components at the gradient level. The background large-scale fields are not barotropic but are baroclinic though the horizontal temperature gradient may not be large because of small Coriolis factor.

Table 1, taken from Lilly (1960), shows the values of dry and moist static stability  $\sigma_d$  and  $\sigma_w$  for the mean hurricane season tropical atmosphere.

sphere. Since the wind fields over the typhoon genesis region are very similar to those over the hurricane genesis region, similar moist static stabilities to those of Lilly (1960) may be observed, as evidenced by Palmen (1948) and Kasahara (1954). Mean upward motions considered to be related to winds over the western North Pacific and the western North Atlantic tropical areas seem to cause similar moist static stabilities over both areas.

Figure 2, taken from Gray (1978), shows the

Table 1: Values of dry and moist static stability for the mean hurricane season tropical atmosphere, after Lilly (1960).

| Pressure (mb.) | $\sigma_d(10^{-3}m.^2mb.^{-2} sec.^{-2})$ | $\sigma_w(10^{-3}m.^2mb.^{-2} sec.^{-2})$ |
|----------------|---|---|
| 950            | 6.04                                      | -9.96                                     |
| 900            | 9.24                                      | -8.00                                     |
| 850            | 12.95                                     | -5.81                                     |
| 800            | 14.85                                     | -5.54                                     |
| 750            | 16.87                                     | -5.40                                     |
| 700            | 18.26                                     | -6.04                                     |
| 650            | 20.7                                      | -6.58                                     |
| 600            | 24.6                                      | -5.31                                     |
| 550            | 28.2                                      | -4.06                                     |
| 500            | 32.0                                      | -2.32                                     |
| 450            | 36.7                                      | -1.30                                     |
| 400            | 39.0                                      | 4.02                                      |
| 350            | 39.3                                      | 8.17                                      |
| 300            | 42.1                                      | 17.92                                     |
| 250            | 43.3                                      | 30.3                                      |
| 200            | 104.2                                     | 96.9                                      |
| 175            | 164.                                      | 159.                                      |
| 150            | 344.                                      | 341.                                      |
| 125            | 788.                                      | 784.                                      |
| 100            | 1837.                                     | 1837.                                     |

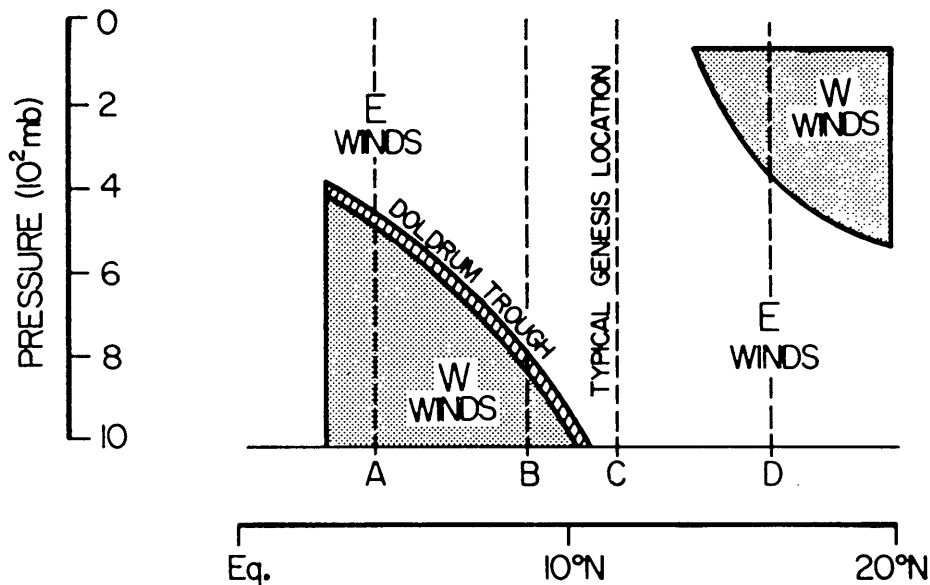


Fig.2: Schematic north-south cross-section of zonal winds relative to the position of a doldrum or monsoon equatorial trough showing easterly shear to the south and westerly shear to the north, reproduced from Gray (1978).

north-south cross-section of zonal wind in the vicinity of the typical typhoon genesis location. Pre-storm cloud clusters tend to be located close to the north of the doldrum trough, south of which is characterized by lower tropospheric westerly winds and upper easterly winds. Therefore, vertical easterly shears are evident in the equatorial latitudes close to the typical genesis location. Pre-storm cloud clusters are located in regions that are almost calm with little shear, although the ambient wave disturbances are influenced by the appreciable vertical shears.

### 1.3 Some aspects of synoptic-scale wave disturbances

N, T and S refer to the ridge, north wind, trough and south wind of the wave defined by the lower tropospheric structure of the mean wave respectively. The meridional wind speed of about  $2.5 \text{ m sec}^{-1}$  seems characteristic of the wave disturbances that traversed the area located around  $10^\circ\text{N}$  where  $f = 0.25 \times 10^{-4} \text{ sec}^{-1}$ . The horizontal characteristic scale  $L_H$  is taken as  $\sim 1000 \text{ km}$  by assuming a quarter of the mean wavelength, as has been suggested, to be  $3800 \text{ km}$ . The waves are finally characterized by the Rossby number given by

$$R_o = \frac{V}{f L_H} \sim 0.1 \quad (1)$$

This Rossby number is one order smaller than

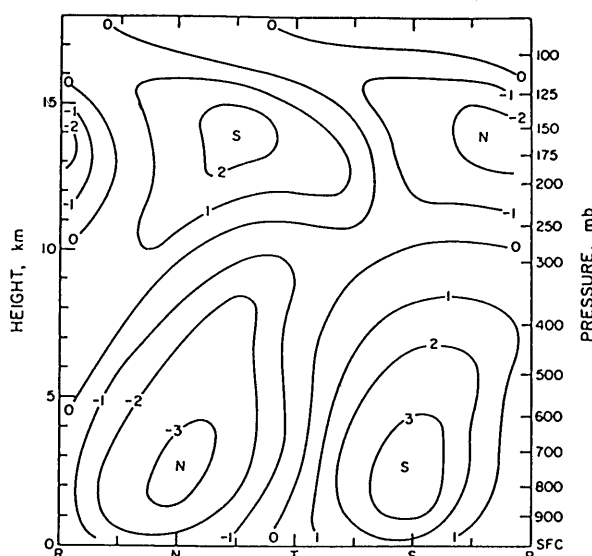


Fig.3: Composite diagram of meridional wind speed ( $\text{m sec}^{-1}$ ) for the network of Kwajalein, Eniwetok and Ponape. The letters R, N, T and S refer to the ridge, north wind, trough and south wind regions, respectively, of the wave as defined by its structure in the lower troposphere, reproduced from Reed and Recker (1971).

Figure 3, taken from Reed and Recker (1971), shows a composite diagram of the meridional wind speed (in  $\text{m sec}^{-1}$ ) of the synoptic-scale wave disturbances that traversed the equatorial western Pacific triangular area described by Kwajalein, Eniwetok and Ponape with an interval of 5 days and an average wave speed of  $7^\circ$  of longitude per day. The letters R,

what has been used since Charney (1963) because different  $V$  ( $\sim 10 \text{ m sec}^{-1}$ ) and  $f$  ( $\sim 0.1 \times 10^{-4} \text{ sec}^{-1}$ ) have been used for the same  $L_H$ . The latter estimation  $R_o \sim 1$  seems unrealistic because disturbances with such strong winds ( $\sim 10 \text{ m sec}^{-1}$ ) are rarely observed in the area around  $4^\circ \text{ N}$  where  $f \sim 0.1 \times 10^{-4} \text{ sec}^{-1}$  is valid.

The Richardson number is defined by

$$R_i = \sigma_w / \left( \frac{\partial v}{\partial p} \right)^2 \quad (2)$$

The vertical variation of the meridional wind is about  $3 \text{ m sec}^{-1}$  in the lower layer from 1000 mb to 500 mb. The Richardson number at 750 mb of the lower layer is estimated as  $R_i \sim -150$  by assuming  $\sigma_w = -5.4 \times 10^{-3} \cdot \text{m}^2 \cdot \text{mb}^{-2} \cdot \text{sec}^{-2}$  from Table 1. Similarly,  $R_i$  at 250 mb of the upper layer is estimated as  $R_i \sim 300$ .

It is now possible to assume that the tropical synoptic-scale wave disturbances are characterized by  $|R_o R_i| > 10$  at 750 mb and 250 mb and quasi-geostrophic approximation is used in the vorticity and divergence equations at these levels.

The pseudoadiabatic process provides a good approximation for the moist disturbances

and the pseudoadiabatic thermodynamic equation is applied at the 500 mb level. The moist static stability plays an important role in this pseudoadiabatic process. The hydrostatic assumption is valid for the synoptic-scale wave disturbances according to Syono (1953). In this assumption,  $L_v \ll L_H$  is required where  $L_v$  is the vertical characteristic scale.

Figure 4 is a typical picture taken by the Geostationary Meteorological Satellite (GMS) showing excitement of upper tropospheric wave disturbances by cut-off lows like the one labeled C in the mid-oceanic planetary trough. Anticyclonic vortexes of the upper tropospheric Sub-Equatorial Ridge (SER), south of the wavy streak of cirrus, are intensified by this sort of cut-off low. Shimizu (1983) has shown several waves of this sort propagated westward

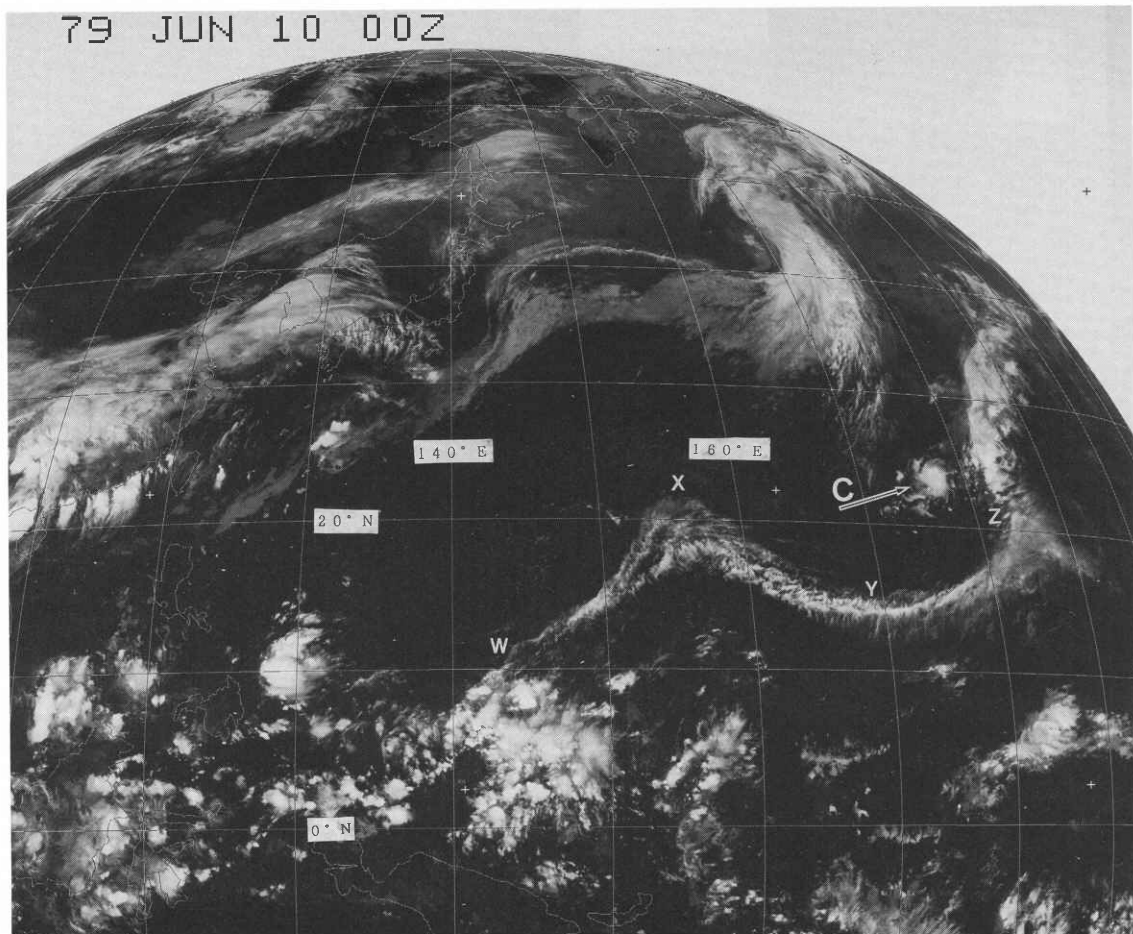


Fig.4: Infrared picture of GMS at 00 UTC June 10 1979. Cirrus streak along W~X~Y~Z suggests an upper tropospheric synoptic-scale wave likely caused by cut-off lows such as C.

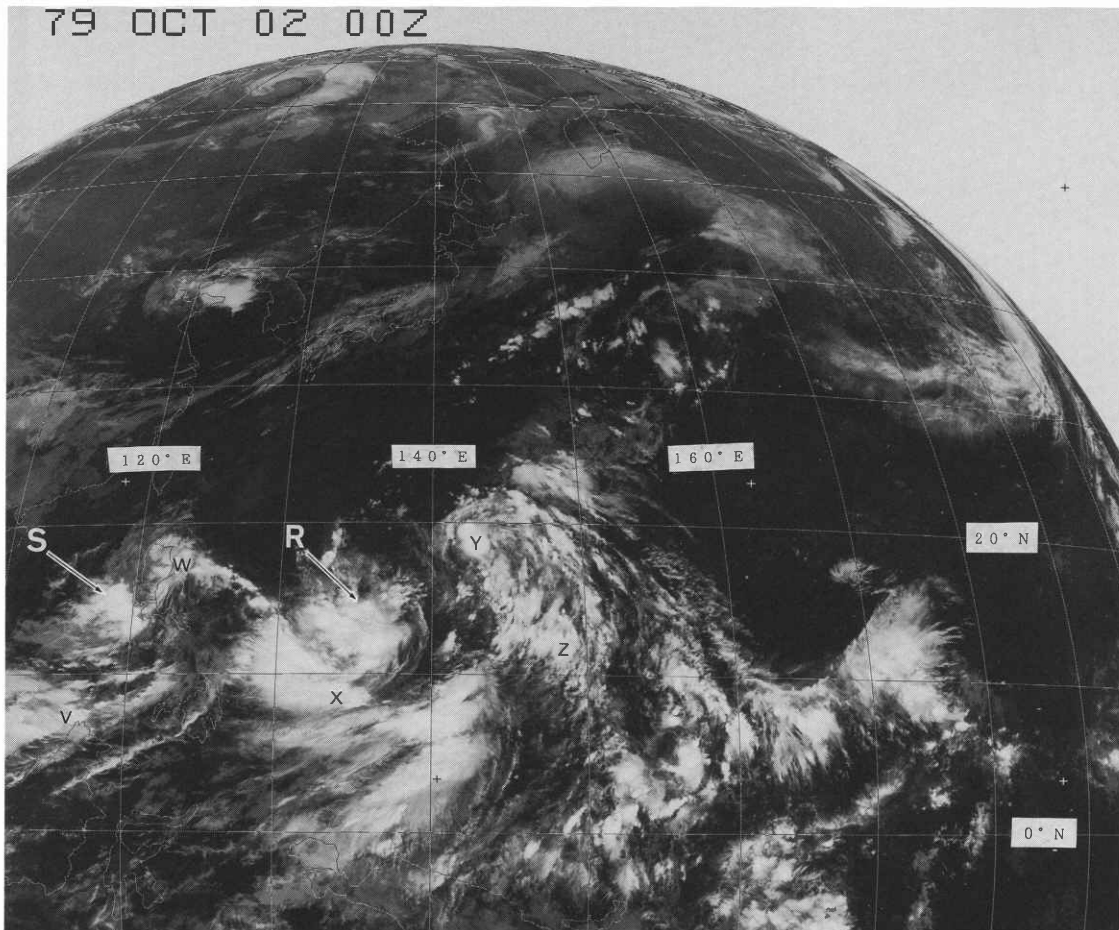


Fig.5: Infrared picture of GMS at 00 UTC Oct. 2 1979. Cloud band along V~W~X~Y~Z suggests existence of synoptic-scale wave disturbance. Mesoscale cloud clusters S (later tropical storm 19 Sarah 1979) and R (later tropical storm 18 Roger 1979) are coexistent near the centers of the cyclonic curvature of the cloud band.

from mid September to early October of 1979. The wavelength and the period seemed to be about 2000 km and 5 days, respectively. A typical ITCZ wave disturbance shown in Figure 5 seemed to develop in response to upper tropospheric disturbances. The horizontal scales of cloud clusters S and R are about a few hundred km and the spacing between them is about 2000 km. These are two characteristic scales in this ITCZ wave disturbance. If cloud patterns are almost quasi-stationary, the dispersion velocities of the respective components should be almost the same.

#### 1.4 Objects of present tentative view

The present view aims at synoptic understanding of the genesis and development of

tropical disturbances in convectively unstable atmosphere with vertical shears of zonal winds. Particular attention is paid to the possible role of upper tropospheric wave disturbances in the development of ITCZ wave disturbances. Combined pseudoadiabatic and quasi-geostrophic approximation is used for the disturbances in the ITCZ as well as hydrostatic approximation. These assumptions seem realistic and provide us with an understanding of the development of tropical disturbances.

Basic equations are given in section 2. The development of synoptic-scale wave disturbances is discussed in section 3 by use of two level model. Development of cloud cluster-scale disturbances is discussed in section 4. Preferential vertical easterly shear over wester-

ly shear is stressed in the development of tropical disturbances in section 5. The results are summarized in section 6.

## 2. Basic Equations

The equation of state of the moist air with pressure  $p$ , specific volume  $\alpha$ , temperature  $T$  and mixing ratio  $q$  is given by,

$$P \alpha = R_m T, \quad (3)$$

where  $R_m$  is the gas constant of the moist air and is related to the gas constant of the dry air  $R_d$  as given by

$$R_m = (1 + 0.608q)R_d. \quad (4)$$

$R_m$  is greater than  $R_d$  by only about 2 percent even if  $q$  is 30 g/kg. The equation of state, however, will not appear in the following discussion, because it has been used implicitly.

The thermodynamic equation for moist air disturbance in a pseudoadiabatic process is given by

$$\left(\frac{\partial}{\partial t} + \mathbf{V} \cdot \nabla\right) \alpha - \sigma \omega = 0 \quad (5)$$

where  $\mathbf{V}$  is the horizontal velocity,  $\omega$  the vertical  $p$ -velocity,  $t$  the time and  $\sigma$  the moist static stability defined by

$$\sigma = -\alpha \frac{\partial \ln \theta_e}{\partial p} \quad (6)$$

where  $\theta_e$  is the equivalent potential temperature.

The hydrostatic approximation is assumed and is given by

$$\frac{\partial \phi}{\partial p} + \alpha = 0 \quad (7)$$

where  $\phi$  is the geopotential. Disturbances whose horizontal scale  $L_H$  and vertical scale  $L_V$  satisfy the condition that  $L_H/L_V \gg 1$ , are considered under this hydrostatic approximation.

So, discussion will be made on disturbances which are characterized by  $L_V \sim 10$  km and  $L_H \geq 100$  km. Under the hydrostatic approximation, the pressure coordinates  $(x, y, p, t)$  are used where  $x$  is eastward and  $y$  northward, and  $p$  decreases upward. The equation of continuity is given by

$$\nabla \cdot \mathbf{V} + \frac{\partial \omega}{\partial p} = 0. \quad (8)$$

The vorticity equation under quasi-geostrophic approximation is given by

$$\frac{\partial \xi}{\partial t} + \mathbf{V}_\psi \cdot \nabla (\xi + f) + f_0 \nabla \cdot \mathbf{V} = 0 \quad (9)$$

where  $\xi$  is the relative vorticity,  $\mathbf{V}_\psi$  is the nondivergent wind and  $f_0$  is the Coriolis factor at the latitude in question. The divergence equation under quasi-geostrophic approximation is given by

$$f_0 \nabla^2 \psi - \nabla^2 \phi = 0 \quad (10)$$

where  $\psi$  is the stream function.

## 3. Development of synoptic-scale wave component

### 3.1 Linearized equations

Putting  $\mathbf{v} = U \mathbf{i} + v \mathbf{j}$ , where  $\mathbf{i}$  and  $\mathbf{j}$  are eastward and northward unit vectors, respectively, and  $U$  and  $v$  are mean zonal wind and disturbed meridional wind, respectively. We get two linearized equations on a  $\beta$ -plane;

$$\left(\frac{\partial}{\partial t} + U \frac{\partial}{\partial x}\right) \frac{\partial^2 \psi}{\partial x^2} + \beta \frac{\partial \psi}{\partial x} - f_0 \frac{\partial \omega}{\partial p} = 0, \quad (11)$$

$$\left(\frac{\partial}{\partial t} + U \frac{\partial}{\partial x}\right) \frac{\partial \psi}{\partial p} - \frac{\partial U}{\partial p} \frac{\partial \psi}{\partial x} + \frac{S}{f_0} \omega = 0, \quad (12)$$

and

$$S = -A \frac{\partial \ln \Theta_e}{\partial p} \quad (13)$$

where  $A$  and  $\Theta_e$  are the mean specific volume

and the mean equivalent potential temperature, respectively, and  $S$  is the mean moist static stability, similar to  $\sigma_w$  in Table 1.

### 3.2 Linear analysis of motion in two-level model

An atmospheric model is shown in Figure 6 with a negative zonal wind  $U_1$  and a positive zonal wind  $U_3$  at upper and lower levels 1 and 3, respectively. Therefore, it has a negative vertical shear  $\Delta U$ . A schematic vertical distribution of the moist static stability is shown by the  $S \sim S$  curve which is negative in the lower levels 4 and 3, slightly negative at the middle level 2, positive at level 1 and very large at level 0. The p-velocity  $\omega$  is assumed to vanish at levels 0 and 4.

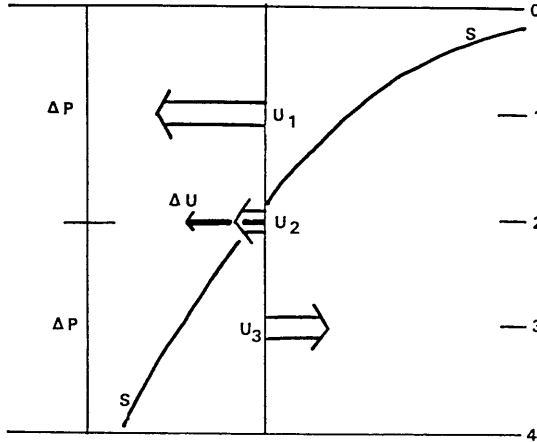


Fig.6: A model atmosphere having vertical easterly shear with upper negative wind  $U_1$  and lower positive wind  $U_3$ . Moist static stability is shown by  $S \sim S$  which is negative in the lower layer, positive in the upper layer and slightly negative at middle level 2.

The linearized vorticity equation is applied at levels 1 and 3, and the linearized thermodynamic equation is applied at level 2. The actual vertical shear is not homogeneous but it is assumed to be independent of  $y$  (i.e., the meridional coordinate). The perturbations are also assumed to be independent of  $y$  and are described by

$$\left(\frac{\partial}{\partial t} + U_1 \frac{\partial}{\partial x}\right) \frac{\partial^2 \psi_1}{\partial x^2} + \beta \frac{\partial \psi_1}{\partial x} - \frac{f_0}{\Delta p} \omega_2 = 0 \quad (14)$$

$$\left(\frac{\partial}{\partial t} + U_3 \frac{\partial}{\partial x}\right) \frac{\partial^2 \psi_3}{\partial x^2} + \beta \frac{\partial \psi_3}{\partial x} + \frac{f_0}{\Delta p} \omega_2 = 0 \quad (15)$$

$$\left(\frac{\partial}{\partial t} + U_2 \frac{\partial}{\partial x}\right) (\psi_1 - \psi_3) - \Delta U \frac{\partial}{\partial x} (\psi_1 + \psi_3) - \frac{S \Delta p}{f_0} \omega_2 = 0 \quad (16)$$

where

$$U_2 = \frac{U_1 + U_3}{2} \quad \text{and} \quad \Delta U = \frac{U_1 + U_3}{2} \quad (17)$$

Let  $\psi_1$  be the triggering upper wind disturbance at level 1, and  $\psi_3$  and  $\omega_2$  be the corresponding wind disturbance at level 3 and vertical p-velocity at level 2, respectively, which are excited by  $\psi_1$ . The wave forms with wavenumber  $k$  are assumed for them

$$\begin{bmatrix} \psi_1 \\ \omega_2 \\ \psi_3 \end{bmatrix} = \begin{bmatrix} \Psi_1 \\ \Omega_2 \\ \Psi_3 \end{bmatrix} e^{ik(x-ct)} \quad (18)$$

where  $\Psi_1$ ,  $\Omega_2$  and  $\Psi_3$  are the amplitudes of  $\psi_1$ ,  $\omega_2$  and  $\psi_3$  respectively, and  $c$  is the imaginary phase speed of the waves given by  $c = c_r + ic_i$  where  $i$  is the unit imaginary number.

Substitution of Eq. (18) into Eqs. (15) – (17) gives

$$ik [(c - U_1) k^2 + \beta] \Psi_1 - \frac{f_0}{\Delta p} \Omega_2 = 0 \quad (19)$$

$$ik [(c - U_3) k^2 + \beta] \Psi_3 + \frac{f_0}{\Delta p} \Omega_2 = 0 \quad (20)$$

$$-ik(c - U_3) \Psi_1 + ik(c - U_1) \Psi_3 - \frac{S_2 \Delta p}{f_0} \Omega_2 = 0 \quad (21)$$

For nonzero  $\Psi_1$ ,  $\Omega_2$  and  $\Psi_3$  to exist,

$$c_r = U_2 - \frac{\beta (k^2 + \lambda^2)}{k^2 (k^2 + 2\lambda^2)} \quad (22)$$

$$c_i = \frac{\sqrt{(4\lambda^4 - k^4)k^4(\Delta U)^2 - \beta^2 \lambda^4}}{k^2 (k^2 + 2\lambda^2)} \quad (23)$$

where



$$\lambda^2 = \frac{f_0^2}{S_2 (\Delta p)^2} \quad (24)$$

This treatment is for tropical disturbances in the atmosphere with negative moist static stability but is similar to those of Phillips (1954), Haltiner (1970) and Holton (1979) for extratropical disturbances in the atmosphere with positive dry stable static stability.

### 3.3 Dynamic instability of the vertical shear in convectively unstable tropics

It is clear that  $\lambda^2$  can be negative when  $S_2$ , the mean moist static stability at level 2, is also negative. Actual phase speeds of the wave components of a disturbance depend on  $k^2$ ,  $\lambda^2$  and  $\beta$  as well as  $U_2$ . The second term of the right hand side of Eq. (22), which is referred to as  $D$  here, is dispersive depending on  $k^2$  at certain values of  $\lambda^2$  and  $\beta$ . Figure 5 shows that synoptic-scale wave disturbances with a wavelength about 2000 km coexist with two cloud masses, S and R with a horizontal scale of about 200 km. Their coexistence requires the condition  $S_2 = -0.26 \times 10^{-3} \text{ m}^2 \cdot \text{mb}^{-2} \cdot \text{sec}^{-2}$  as will be discussed in section 5. Figure 7 shows the changes in  $D$  against wavelength  $L$  at  $10^\circ\text{N}$  with  $\Delta p = 500 \text{ mb}$  and the same value of  $S_2$ . Waves with  $L$  longer than  $L_{qs}$  (wavenumber  $k_{qs}$  satisfies  $k_{qs}^2 + \lambda^2 = 0$ ) disperse westward. While waves with  $L$  shorter than  $L_{qs}$  and longer than asymptotic wavelength  $L_{cr}$  (wavenumber  $k_{cr}$  satisfies  $k_{cr}^2 + 2\lambda^2 = 0$ ) disperse eastward. The waves in this range may move eastward, if  $U_2$  is small. Waves with  $L$  shorter than  $L_{cr}$  disperse westward. The dispersion of cloud clusters, the scale of which is a few hundred km, is close to zero. This strongly suggests that the cloud clusters coexist with the synoptic-scale wave that fulfills  $L=L_{qs}$ . This also accounts for the experimental law that a tropical disturbance, being composed of a synoptic-scale

wave component and a few mesoscale wave components like cloud clusters, are steered by steering winds at a middle tropospheric level.

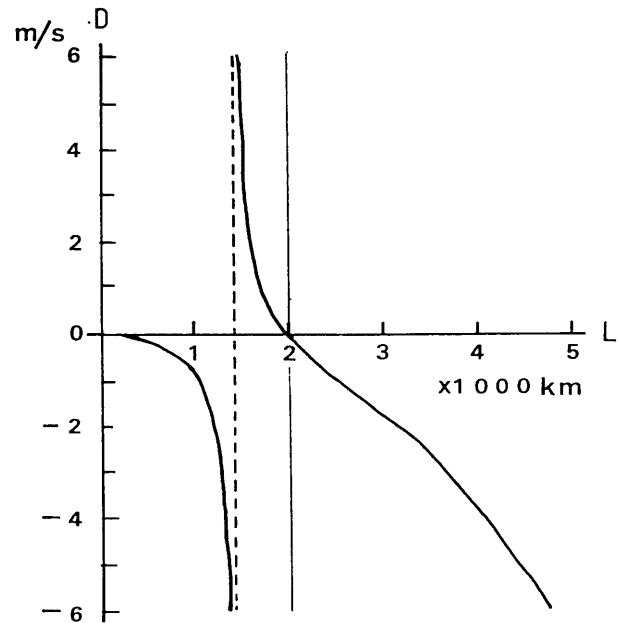


Fig.7: Dispersion velocity  $D$  as a function of wavelength  $L$  for  $S_2 = -0.25 \times 10^{-3} \text{ m}^2 \cdot \text{mb}^{-2} \cdot \text{sec}^{-2}$ . Broken and thin lines show the critical wavelength and quasi-stationary wavelength, respectively.

Figure 8 shows a dynamic stability diagram with the wavelength in thousands of km as the abscissa, and half the absolute value of the wind difference between the upper tropospheric level (assumed to be 250 mb) and the lower level (assumed to be 750 mb) as the ordinate. The same moist static stability  $-0.26 \times 10^{-3} \text{ m}^2 \cdot \text{mb}^{-2} \cdot \text{sec}^{-2}$  as in Fig.7 is used. The latitude is also taken as  $10^\circ\text{N}$ . Unstable waves are longer than the critical wavelength. If the moist static stability becomes close to zero, then the critical wavelength becomes shorter. This dynamic stability diagram is similar to that given for middle latitude disturbances in the standard atmosphere with the positive static stability as instructed by Haltiner (1970). It should be noted that the dynamic stability is apparently independent of the signs of the moist static stability, the vertical shear and the Coriolis factor.

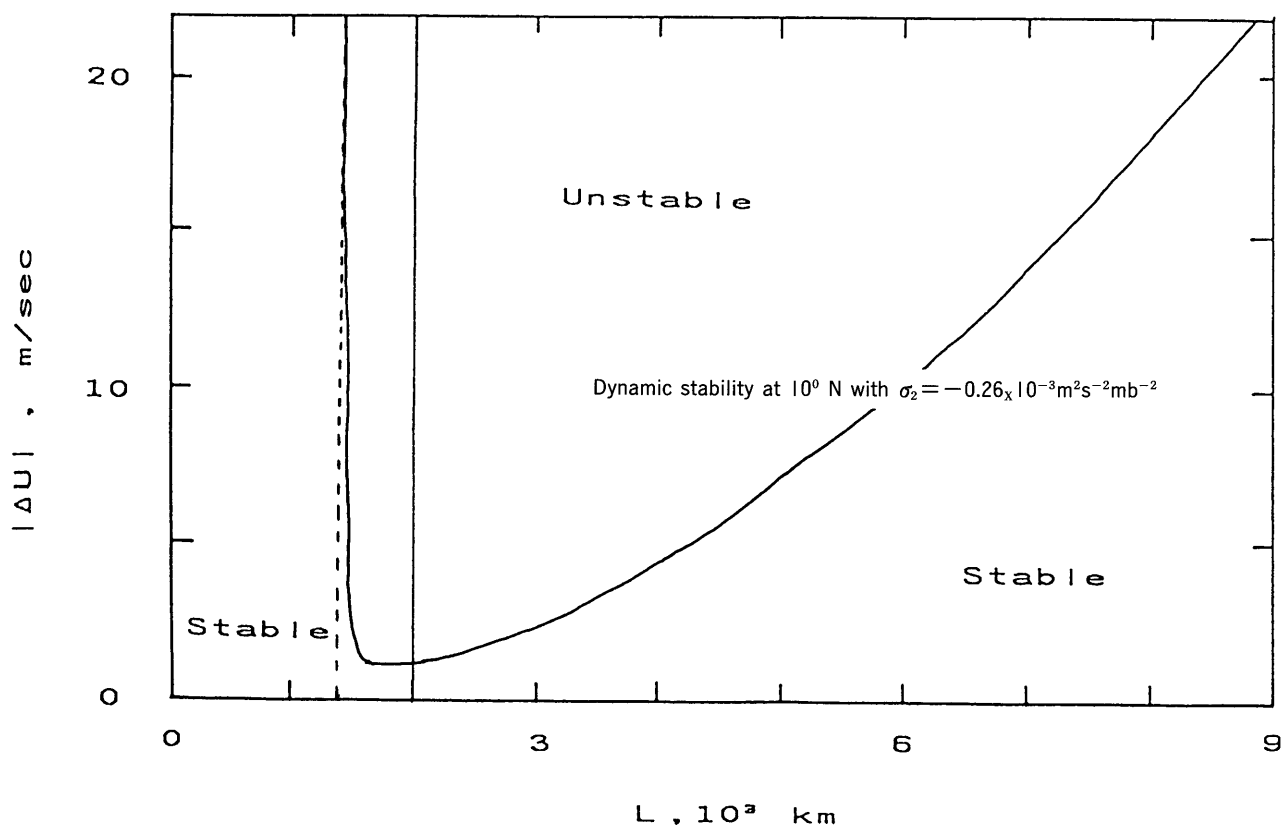


Fig.8: Dynamical stability diagram for  $10^\circ\text{N}$  with  $S_2 = -0.26 \times 10^{-3} \text{ m}^2 \cdot \text{mb}^{-2} \cdot \text{sec}^{-2}$  against wavelength  $L$  and the absolute value of  $\Delta U$  illustrated in Fig.6. Broken and thin lines show critical wavelength and quasi-stationary wavelength, respectively.

#### 4. Development of cluster-scale upward motion in doldrums

A synoptic-scale tropical disturbance has its characteristic cloud cluster in the core region where winds are typically very weak. The cloud cluster is a mesoscale disturbance which is not allowed to grow by baroclinic instability, as already shown in previous Fig.8. The mechanism of development of the cloud cluster should be investigated.

Perturbations in a rest state are described by

$$\frac{\partial \mathbf{V}}{\partial t} + f_0 \mathbf{k} \times \mathbf{V} + \nabla \phi = 0 \quad (25)$$

and

$$\frac{\partial \alpha}{\partial t} - S \omega = 0 \quad (26)$$

Using Eqs. (7), (8), (25) and (26), we get

$$\left( \frac{\partial^2}{\partial t^2} + f_0^2 \right) \frac{\partial^2 \omega}{\partial p^2} + S \frac{\partial^2 \omega}{\partial x^2} = 0 \quad (27)$$

At the top and the bottom of the troposphere,  $\omega$  is assumed to disappear and is assumed to take the form

$$\omega = \Omega e^{nt} e^{imx} \quad (28)$$

where  $m$  is the wavenumber of a mesoscale cloud cluster and  $n$  is the growth rate. Putting Eq. (28) into Eq. (27), we have:

$$(n^2 + f_0^2) \frac{d^2 \Omega}{dp^2} - m^2 S \Omega = 0 \quad (29)$$

Now that  $S$  is a function of  $p$ , Eq. (29) is solved by a difference method using the two-level model shown in Figure 6, though the zonal winds are assumed to be zero in the present case. The following relation is obtained for nonzero  $\Omega$  to exist:

$$n = \sqrt{-(f_0^2 + \frac{m^2 (\Delta p)^2 S_2}{2})} \quad (30)$$

If the condition  $n > 0$  is satisfied and any initial trigger  $\Omega_2$  is given, upward motions with wavenumber  $m$  will grow. The wave number  $m$  is not necessarily equal to the synoptic-scale wave number. For  $n$  to be positive,

$$S_2 < -\frac{2 f_0^2}{m^2 (\Delta p)^2} \quad (31)$$

must be fulfilled. Let  $f_0 \sim 0.25 \times 10^{-4} \cdot \text{sec}^{-1}$ ,  $\Delta p \sim 500 \text{ mb}$  and  $m \sim 3.14 \times 10^{-5} \text{ m}^{-1}$  ( $L \sim 200 \text{ km}$ ), then we obtain the right hand critical static stability  $S_{cr} \sim -0.005 \times 10^{-3} \text{ m}^2 \cdot \text{mb}^{-2} \cdot \text{sec}^{-2}$ . It is possible that the actual  $S_2 \sim -0.26 \times 10^{-3} \text{ m}^2 \cdot \text{mb}^{-2} \cdot \text{sec}^{-2}$ , adopted in the previous section, satisfies the requirement of Eq. (31).

It seems likely that, in the cloud cluster-scale, upward motion develops due to the vertical thermal instability. This instability seems sensitive to variation of moist static stability. If we let  $\delta\sigma_2$  be its mesoscale variation from  $S_2$ , we get

$$\sigma_2 = S_2 + \delta\sigma_2 \quad (32)$$

Then we obtain

$$\delta n = -\frac{m^2}{4n} (\Delta p)^2 \delta\sigma_2 \quad (33)$$

Using Eq. (6) and considering that the equivalent potential temperature is conserved in the pseudoadiabatic process, we obtain

$$\frac{\partial \sigma_2}{\partial t} = -\left[\left(\frac{\partial \alpha}{\partial p} + \sigma\right) \frac{\partial \ln \theta_e}{\partial p} + \frac{\partial \sigma}{\partial p}\right]_{p_2} \omega_2 + \sigma_2 \nabla \cdot \mathbf{V}_2 \quad (34)$$

Since  $\ln \theta_e / \partial p$ ,  $\sigma$  and  $\nabla \cdot \mathbf{V}_2$  are actually small at the middle tropospheric level, we obtain

$$\delta\sigma_2 \sim -\left[\frac{\partial \sigma}{\partial p}\right]_{p_2} \omega_2 \delta t \quad (35)$$

Since  $[\partial \sigma / \partial p]$  is negative at  $p=p_2$ ,  $\sigma_2$  decrease in association with negative  $\omega_2$ . The decrease

of  $\sigma_2$  causes positive  $\delta n$  to intensify  $\omega_2$  recurrently. This strongly suggests that mesoscale cloud clusters in convectively unstable atmosphere develops spontaneously if the initial motions are triggered by synoptic-scale motions.

The intensified mesoscale upward motion in the doldrums where the zonal wind  $U$  is very small intensifies the relative vorticity at the lower troposphere and weakens it at the upper troposphere in the following manners:

$$\frac{\partial \xi_3}{\partial t} \sim -\frac{f_0}{\Delta p} \omega_2 \quad (36)$$

and

$$\frac{\partial \xi_1}{\partial t} \sim \frac{f_0}{\Delta p} \omega_2 \quad (37)$$

The intensified mesoscale upward motion warms the convectively unstable tropospheric layer according to,

$$\frac{\partial \alpha_2}{\partial t} \sim \sigma_2 \omega_2 \quad (38)$$

Since the product of  $\sigma_2$  and  $\omega_2$  becomes enormously positive, appreciable warming can take place locally in the convectively unstable tropospheric layer in the doldrums if a mesoscale convective cloud cluster is present.

## 5. Discussion

According to a well-known synoptic law, synoptic-scale tropical disturbances have the steering level in a middle tropospheric layer. This suggests that the following relations are fulfilled:

$$c_r \sim U_2 \quad \text{and} \quad k^2_{qs} + \lambda^2 \sim 0 \quad (39)$$

where  $U_2$  is regarded as an approximate steering wind. A wave disturbance can be quasi-stationary with respect to the coordinate moving with  $U_2$  if the wavenumber fulfills the latter approximation. The corresponding

wavelength  $L_{qs}$  is approximated by

$$L_{qs} \sim 2 \pi \Delta p \frac{\sqrt{-S_2}}{|f_0|} \quad (40)$$

Table 1, after Lilly (1960), suggests  $S_2 \sim -2.32 \times 10^{-3} \text{ m}^2 \cdot \text{mb}^{-2} \cdot \text{sec}^{-2}$  in areas of hurricane activity around  $20^\circ\text{N}$  with  $f_0 \sim 0.5 \times 10^{-4} \text{ sec}^{-1}$ . These values give  $L_{qs} \sim 3000 \text{ km}$  if  $\Delta p \sim 500 \text{ mb}$  is used. An ITCZ wave disturbance shown by Agee (1972) seems to have this wavelength. While  $L_{gs} \sim 2000 \text{ km}$  is suggested in the ITCZ wave disturbance in the area of typhoon activity around  $10^\circ\text{N}$  as shown in Fig.5, then  $S_2 \sim -0.26 \times 10^{-3} \text{ m}^2 \cdot \text{mb}^{-2} \cdot \text{sec}^{-2}$  is suggested in this area. This value of  $S_2$  was used in deriving Figs 7 and 8.

Putting  $c \sim U_2 + iG/k_{qs}$  where  $G$  is the growth rate, we get

$$\psi_3 \sim \frac{k_{qs}^2 \Delta U - \beta - ik_{qs} G}{k_{qs}^2 \Delta U + \beta + ik_{qs} G} \psi_1 \quad (41)$$

and

$$\omega_2 \sim \frac{ik_{qs} \Delta p}{f_0} [-k_{qs}^2 \Delta U + \beta + ik_{qs} G] \psi_1 \quad (42)$$

Eq. (41) shows the response of  $\psi_3$  to  $\psi_1$ . The growth rate  $G$  of the quasi-stationary wave with  $k=k_{qs}$  are known if  $v_1 (=ik\psi_1)$ ,  $v_3 (=ik\psi_3)$  and  $\Delta U$  are given by numerical predictions. Eq. (42) shows the response of  $\omega_2$  to  $\psi_1$ . The value of  $\omega_2$  is evaluated if  $\Delta U$ ,  $G$  and  $\psi_1$  are given. If  $\Delta U = \sim 1.3 \text{ m/s}$ ,  $G = \sim 2.0 \times 10^{-5} \text{ s}^{-1}$  ( $\sim 14$  hours of e-folding time) and  $v_1 = \sim 2.5 \text{ m/s}$  are given,  $\omega_2 = \sim 130 \times 10^{-5} \text{ mb/s}$ , which is similar to the vertical p-velocity estimated by Reed and Recker (1971). If the daily genesis potential of tropical cyclone is defined by  $DGP = \xi_3 - \xi_1$  similarly to McBride and Zehr (1981), it is given by

$$DGP = 2 k^2 \frac{\beta + ikG}{k^2 \Delta U + \beta + ikG} \psi \quad (43)$$

Eq. (43) gives estimation of DGP if  $\Delta U$ ,  $G$  and  $\psi_1$  are given which is very useful in predicting genesis of tropical cyclone.

Considering the simplest case where  $G \sim 0$  is valid, we get

$$3 k^4 (\Delta U)^2 - \beta^2 \sim 0 \quad (44)$$

In this simple case, it is suggested that the response of  $\psi_3$  to  $\psi_1$  for  $\Delta U < 0$  is about 14 times as large as that for  $\Delta U > 0$ . Strong low level winds tend to respond to triggering upper level winds in the case of easterly shear rather than westerly shear. The response of  $\omega_2$  to  $\psi_1$  when  $\Delta U < 0$  is about 4 times larger than for  $\Delta U > 0$ . The DGP for easterly shear is about 4 times larger than for westerly shear.

These relations clearly explain why tropical storms originate preferentially in the western North Pacific and western North Atlantic where vertical easterly shears are more frequent due to the Tibetan and the Mexican Plateaus, respectively. These shears, as well as atmospheric convective instability, are more likely to lead to tropical cyclogenesis.

CISK is generally accepted by meteorologists as necessary dynamic and thermodynamic process for tropical cyclone formation, but CISK calculationa are based on the initial disturbance which has not yet been explained. Synoptic-scale wave disturbances which develop through this dynamic instability may trigger the CISK mechanism. In this paper, we focused on the role of upper tropospheric wave disturbances that are mostly caused by cut-off lows in the mid-oceanic planetary trough region.

Dynamic and thermodynamic background of CISK was explained clearly. A reciprocal process was found between decreased moist

static stability due to upward motion and increased upward motion due to decreased moist static stability. This reciprocal process clearly induces a local warm core in the region of intense upward motion. If we introduce  $m$  for mesoscale wavenumber in stead of  $k_{qs}$  in Eq. (41), we get

$$\psi_3 = \frac{m^2 \Delta U - imG}{m^2 \Delta U + imG} \psi_1 \quad (45)$$

where  $\beta$  was omitted in comparison with the other two terms. It is clear that  $\psi_3 \sim -\psi_1$  if  $\Delta U \sim 0$ . This inverse phase difference suggests warm air between them.

## 6. Summary

A tentative view was presented concerning development of tropical disturbances in the western North tropical Pacific area where the atmosphere is convectively unstable and has vertical easterly shear. Adoption of realistic moist static stability and characteristic wind allowed us to use pseudoadiabatic and quasi-geostrophic approximation for the synoptic-scale wave disturbances.

The synoptic-scale disturbances were found to develop due to the dynamic instability of the vertical wind shear in the convectively unstable tropical atmosphere. Preference of easterly shear over westerly shear was found to generate tropical cyclones.

Cluster-scale disturbances in convectively unstable atmosphere in the doldrums were found to develop spontaneously because upward motions are intensified by decreases of moist static stability and the decreases of the moist static stability are, in turn, caused by the intensified upward motions. This reciprocal process causes the formation of the warm core of tropical disturbance. It also induces strong cyclonic vorticity at the lower level and anticyclonic

vorticity at the upper level of the troposphere.

## Acknowledgments

The author would like to thank to Mr. Yukizo Sano, the Director General of the Meteorological Satellite Center, for his encouragement and comments about the manuscript. He also would like to thank to Mr. Yoshiaki Takeuchi for his invaluable comments and advices for improving the manuscript and to members of the center for their fruitful discussions.

## References

- Agee, E. M., 1972: Note on ITCZ wave disturbances and formation of tropical storm Anna. *Mon. Wea. Rev.*, **96**, 106-117.
- Charney, J. C., 1963: A note on large-scale motions in the tropics. *J. Atmos. Sci.*, **20**, 607-609.
- and A. Eliassen, 1964: On the growth of hurricane depression. *J. Atmos. Sci.*, **21**, 68-75.
- Frank, W. M., 1977: The structure and energetics of the tropical cyclone. I. Storm structure. *Mon. Wea. Rev.*, **105**, 1119-1135.
- Gray, W. M., 1968: Global view of the origin of tropical disturbances and storms. *Mon. Wea. Rev.*, **96**, 669-699.
- , 1978: Hurricanes: Their formation, structure and likely role in the tropical circulation. *Meteorology over the tropical oceans*. *Roy. Met. Sci.*, 155-218.
- Haltiner, G. J., 1971: Numerical weather prediction. 317 pp, John Wiley & Sons, Inc. New York London Sydney Toronto.
- Holton, J. R. 1979: An introduction to dynamic meteorology. 2nd edition. 319 pp, Academic Press, New York San Francisco London.
- Kasahara, A., 1954: Supplementary notes on the formation and the schematic structure of

- typhoons. J. Met. Soc. Japan, **32**, 31-52.
- , 1960: The development of forced convection caused by the released latent heat of condensation in a hydrostatic atmosphere. Proceedings of the International Symposium on Numerical Weather Prediction in Tokyo. 387-403, Met. Soc. Japan.
- Lee, C. S., 1989: Observational analysis of tropical cyclogenesis in the western North Pacific. Part I: Structure evolution of cloud clusters. J. Atmos. Sci., **46**, 2580-2598.
- Lilly, D. K., 1960: On the theory of disturbances in a conditionally unstable atmosphere. Mon. Wea. Rev., **88**, 1-17.
- McBride, J.L. and R. Zehr, 1981: Observational analysis of tropical cyclone formation. Part II: Comparison of non-developing versus developing systems. J. Atmos. Sci., **38**, 1132-1150.
- Ooyama, K., 1964: A dynamical model for the study of tropical cyclone development, paper presented at 3rd Tech. Conf. on Hurricanes and Trop. Meteorol., Mexico City.
- Palmen, E., 1948: On the formation and structure of tropical hurricanes. Geophysica, **3**, 26-38.
- Phillips, N. A., 1954: Energy transformations and meridional circulations associated with simple baroclinic waves in a two-level, quasi-geostrophic model. Tellus, **6**, 273-286.
- Reed, R. J. and R. E. Recker, 1971: Structure and properties of synoptic-scale wave disturbances in the equatorial western Pacific. J. Atmos. Sci., **28**, 1117-1133.
- Shimizu, N. 1983: Westward propagation of upper tropospheric wind disturbances during the mid-season of typhoon development of 1979. Geophys. Mag., **40**, 297-312.
- Shono, S. 1953: On the formation of tropical cyclones. Tellus, **5**, 179-195.
- 1960: A numerical experiment of the formation of tropical cyclones. Proceedings of the International Symposium on Numerical Weather Prediction in Tokyo. 405-418, Met. Soc. Japan.
- Yanai, M., 1961: A detailed analysis of typhoon formation. J. Met. Soc. Japan, **39**, 187-214.
- , 1964: Formation of tropical cyclones. Rev. Geophys., **2**, 367-414.

## 熱帯擾乱の発達に関する一見解

清水喜允

気象衛星センター

多くの場合切離低気圧によって準赤道リッジ域に形成される上部対流圏の総観規模の波動が、西風シアーよりはむしろ東風シアーが卓越する地域で、下部対流圏及び中部対流圏にも擾乱を誘起する。この総観規模の擾乱は東西風の鉛直シアーの力学的不安定によって発達する。

雲クラスター規模の運動は上記の総観規模の波動の中心地域で相助的に発達する。すなわち、上昇流は湿潤静的安定度を減少させ、逆に、その湿潤静的安定度の減少は上昇流を強める。この回帰的な過程は究極的には対流不安定層に暖気核を形成するとともに、下部対流圏には低気圧性うず度を、上部対流圏には高気圧性うず度を形成する。